(2)

OFFICE OF NAVAL RESEARCH

Contract N00014-82-K-0280

Task No. NR413E001

TECHNICAL REPORT NO. 29

PH_3 Surface Chemistry on Si(111)-(7x7) - A Study by Auger Spectroscopy and Electron Stimulated Desorption Methods

by

R.M. Wallace, P.A. Taylor, W.J. Choyke, and J.T. Yates, Jr.

Submitted to

J. Appl. Physics

Surface Science Center
Department of Chemistry
University of Pittsburgh
Pittsburgh, PA 15260

11 April 1990

REPORT DOCUMENTATION PAGE

READ INSTRUCTIONS BEFORE COMPLETING FORM

1. REPORT NUMBER: 29

2. GOVT ACCESSION NO.:

3. RECIPIENT'S CATALOG NUMBER:

4. TITLE (and Subtitle): PH3 Surface Chemistry on Si(111)-(7x7) - A Study by Auger Spectroscopy and Electron Stimulated Desorption Methods

5. TYPE OF REPORT & PERIOD COVERED:

6. PERFORMING ORG. REPORT NUMBER:

7. AUTHOR(s): R.M. Wallace, P.A. Taylor, W.J. Choyke, and J.T.Yates, Jr.

8. CONTRACT OR GRANT NUMBER(s):

9. PERFORMING ORGANIZATION NAME AND ADDRESS: Surface Science Center, Chemistry Department University of Pittsburgh, Pittsburgh, PA 15213

10. PROGRAM ELEMENT, PROJECT, TASK AREA & WORK UNIT NUMBERS:

11. CONTROLLING OFFICE NAME AND ADDRESS:

12. REPORT DATE: 4/11/90

13. NUMBER OF PAGES: 40

14. MONITORING AGENCY NAME & ADDRESS (if different from Controlling Office):

15. SECURITY CLASS. (of this report): Unclassified

15a. DECLASSIFICATION/DOWNGRADING SCHEDULE:

16. DISTRIBUTION STATEMENT (of this Report):

17. DISTRIBUTION STATEMENT (of the abstract entered in Block 20, if different from Report):

18. SUPPLEMENTARY NOTES:

19. KEY WORDS (Continue on reverse side if necessary and identify by block number)

Si(111)
PH_3
Phosphine
Phosphorus

20. ABSTRACT (Continue on reverse side if necessary and identify by block number)

The adsorption and decomposition of PH_3 on Si(111)-(7x7) was investigated in ultrahigh vacuum by means of temperature programmed desorption (TPD), low energy electron diffraction (LEED), Auger electron spectroscopy (AES) and electron stimulated desorption (ESD) methods. Phosphine adsorbs on Si(111)-(7x7) at T=120 K with an initial sticking coefficient of $S_o \approx 1$ through a mobile (extrinsic) precursor state. Some PH_3 dissociative adsorption at 120 K is observed. Thermal activation of the adsorbed species results in desorption of a molecular PH_3 species up to 550 K. Further heating produces $H_2(g)$ desorption at T = 740 K and $P_2(g)$ desorption at T = 1010 K, thus indicating that PH_3 decomposition has occurred. AES and ESD studies of the adsorbed species reveal that decomposition takes place by the breaking of P-H bonds in $PH_x(a)$ to form Si-H species on the surface for 120 K < T < 700 K.

DD FORM 1 JAN 73 1473 EDITION OF 1 NOV 65 IS OBSOLETE

Submitted to: J. Appl. Physics

Date: 11 April 1990

PH_3 Surface Chemistry on Si(111)-(7x7) - A Study by Auger Spectroscopy and Electron Stimulated Desorption Methods

R.M. Wallace, P.A. Taylor, W.J. Choyke,[a] and J.T. Yates, Jr.

Surface Science Center
Department of Chemistry
University of Pittsburgh
Pittsburgh, PA 15260

(Received:)

PH_3 Surface Chemistry on Si(111)-(7x7) - A Study by Auger Spectroscopy and Electron Stimulated Desorption Methods

R.M. Wallace, P.A. Taylor, W.J. Choyke,[a] and J.T. Yates, Jr.

Surface Science Center
Department of Chemistry
University of Pittsburgh
Pittsburgh, PA 15260

Abstract

The adsorption and decomposition of PH_3 on Si(111)-(7x7) was investigated in ultrahigh vacuum by means of temperature programmed desorption (TPD), low-energy electron diffraction (LEED), Auger electron spectroscopy (AES) and electron stimulated desorption (ESD) methods. Phosphine adsorbs on Si(111)-(7x7) at T=120 K with an initial sticking coefficient of $S_0 \approx 1$ through a mobile (extrinsic) precursor state. Some PH_3 dissociative adsorption at 120 K is observed. Thermal activation of the adsorbed species results in desorption of a molecular PH_3 species up to 550 K. Further heating produces H_2(g) desorption at T ≈ 740 K and P_2(g) desorption at T ≈ 1010 K, thus indicating that PH_3 decomposition has occurred. AES and ESD studies of the adsorbed species reveal that decomposition takes place by the breaking of P-H bonds in PH_x(a) to form Si-H species on the surface for 120 K < T < 700 K. Keywords: Si (111), PH3, Phosphine desorption, Adsorption, Silicon, Doping, Surface reactions, Passivation, Semiconductors, Chemisorption

PACS numbers: 82.65.My, 82.30.Lp, 68.10.Jy, 81.15.Gh

I. INTRODUCTION

The study of simple hydrides, such as phosphine, on silicon surfaces is important for technological and fundamental reasons. Phosphorus is commonly used as a substitutional dopant in the production of n-type Si devices.[1] The technological growth processes commonly used in the semiconductor industry, such as chemical-vapor deposition (CVD), are expected to involve many of the fundamental physical and chemical interactions which may be conveniently investigated by the methods of surface science under ultrahigh-vacuum (UHV) conditions.[2] In particular, the introduction of various precursor molecules in these growth processes for device doping or passivation purposes occurs through adsorption and reaction mechanisms readily isolated and studied under such controlled conditions.

Phosphine, a common precursor candidate used in the production of n-type Si epitaxial layers, n-type float zone Si[1], and n-type polycrystalline Si thin films[2], has been the subject of silicon surface science studies since 1967. The low energy electron diffraction (LEED) work of Van Bommel and Meyer on single crystal Si(111) revealed that a variety of surface reconstructions are observed from high temperature adsorption and thermal annealing of layers produced by interaction with PH_3 at $T_{ads} > 773$ K.[3] (Similar LEED results were reported earlier by Lander and Morrison for P_4 adsorption on Si(111)[4]).

Further coverage measurements by Van Bommel and Crombeen[5], using Auger electron spectroscopy (AES) and LEED, indicated that the room temperature adsorption of PH_3 on clean Si(111)-(7x7) resulted in a (7x7) reconstruction with 0.33 P/Si. This reconstruction was observed to be stable to a temperature of 770 K where H_2 was assumed to desorb. Higher adsorption temperatures resulted in a (1x1) phase (1 P/Si) for 770 K < T_{ads} < 790 K and a P-(6 $\sqrt{3}$ x 6 $\sqrt{3}$) phase

(3 P/Si) for 800 K < T_{ads} < 900 K. Further high temperature adsorption resulted in a ($2\sqrt{3}x\sqrt{3}$) surface phase followed by another (1x1) reconstruction. Upon adsorption at T_{ads}=1070 K, a "clean"-(7x7) phase was observed and P was assumed to undergo desorption or diffusion into the bulk.

More recent UHV work by Meyerson and Yu[6,7] and Yu et al.[8] has shown that the saturation coverage of phosphorus from PH_3 adsorption on Si(100)-(2x1) has a strong temperature dependence. Using UPS, SIMS, LEED and AES, they found that PH_3 adsorbs on clean Si(100) with a unity sticking coefficient at room temperature.[6] Furthermore, their high temperature adsorption studies indicate that phosphine dissociates on the surface and hydrogen is evolved leaving P bound to the Si(100) surface. Based on photoemission studies,[6] they conclude that the evolved hydrogen originates from the PH_3(a), and little hydrogen (<10%) is transferred to the surface to form Si-H species. However, the desorption of H_2 at T>673 K, as observed by SIMS, resulted in an increased capacity for subsequent PH_3 adsorption, indicating that active adsorption sites are made available upon H_2 desorption.[7] (This result was also observed earlier by Boonstra in the adsorption of PH_3 on Si powders believed to expose primarily Si(111) planes).[9] Further annealing resulted in a loss of P which was assumed to be the result of P desorption.[6,7]

Further XPS and TDS studies by Yu, et al.,[8] suggested that PH_3 adsorbs "mostly undissociatively" at room temperature on Si(100), and they propose that the phosphine lone pair electrons form two σ-bonds with the Si dimer dangling bonds. Upon heating, a PH_3 desorption feature at T ≈ 548 K was observed and subsequent decomposition of the surface species occurred, leading to bound hydrogen and phosphorus. Further heating resulted in H_2(g) desorption at T ≈ 798 K, suggesting the presence of a monohydride Si-H species produced by PH_3 decomposition. Above 823 K, phosphorus desorption occurred and the desorbing

species was identified as $P_2(g)$.

Our experiments are designed to reinvestigate the kinetics of adsorption and the kinetics of P-H bond scission on Si(111). In addition the behavior of surface phosphorus resulting from PH_3 decomposition has been more carefully studied.

In this experimental study, we use LEED, AES, kinetic uptake measurements, line-of-sight temperature programmed desorption (TPD), and electron stimulated desorption (ESD) to examine the adsorption and decomposition of PH_3 on the Si(111)-(7x7) surface. We find that PH_3 adsorbs at 120 K on Si(111)-(7x7) with unity sticking coefficient through an extrinsic mobile precursor state, and that evidence for some dissociative adsorption at 120 K exists. The thermal activation of the PH_3 + PH_x adsorbate ($x<3$) is examined and two reaction channels are observed: (1) the desorption of a molecular species up to $T\approx550$ K, and (2) decomposition leading to the gradual formation of Si-H species from the breaking of P-H bonds in the $PH_3(a)$ + $PH_x(a)$ species for $T<500$ K. ESD measurements as a function of substrate temperature indicate that the $PH_3(a)$ + $PH_x(a)$ species produce significant H^+ desorption yield and that Si-H surface species are not responsible for a significant portion of the observed H^+ ions. We also report the direct detection by TPD of $H_2(g)$ desorption at $T_{max}\approx740$ K, followed by desorption of $P_2(g)$ at $T_{max}\approx1010$ K.

II. EXPERIMENT

A. General overview

The experiments were conducted in the UHV chamber shown in Fig. 1. The base pressure of the chamber is routinely 3×10^{-11} Torr as determined with a Bayard-Alpert (BA) ionization gauge. Pumping is achieved by a 150 l/s turbo

pump, a 200 l/s integral ion pump and a titanium sublimation pump. The pumping time constant of the system is estimated to be 0.5 s. The system, equipped with scanning AES, two UTI 100-C quadrupole mass spectrometers (QMS) and a digital LEED/ESDIAD (electron-stimulated desorption ion angular distribution) instrument, is described below.

B. Auger measurements

Proceeding from the top of Fig. 1 in a clockwise fashion, the system is equipped with a Varian single-pass CMA scanning Auger electron spectrometer operated in a derivative mode with an integral electron gun operated at 3 keV. The modulation voltage used for all of the measurements reported herein is V_m=5 V p-p. Typical beam currents are $2x10^{-6}$ A in a 0.2 mm diameter spot. This results in an electron flux of $4x10^{16}$ $s^{-1}cm^{-2}$ and this flux is clearly large enough to produce electron beam dissociation of the adsorbate when typical analysis times are considered (~ 120 s). The observed ESD effects, described below, confirm this for the $PH_x(a)(x<3)$ species. Thus, the AES measurements reported here serve as a relative assay of the surface phosphide species produced by electron beam degradation of the PH_x surface species present. The observed phosphorus Auger signal is proportional to the phosphorus concentration produced from the electron beam decomposition of the PH_x species. This is consistent with measurements of the P(LVV) Auger intensity increase with increasing PH_3 coverage. An extensive study of the P(LVV) lineshape and intensity showed no changes with prolonged electron beam exposure from the Auger electron gun (up to 7.5 times the typical analysis time).

All AES results reported herein are the result of an average of the peak-to-peak derivative signal intensity made at four locations over the exposed surface of the crystal. With a 0.2 mm diameter AES electron beam spot, a total

area of 0.0003 cm^2 is exposed to the focused beam, thus degrading in four measurements the adsorbed surface species on only 0.07% of the exposed surface. We can therefore conclude that AES and TPD measurements can be conducted together without the production of spurious effects in TPD measurements due to electron beam degradation of an appreciable fraction of the adsorbed layer.

C. Shielded QMS measurements

A differentially-pumped, shielded quadrupole mass spectrometer (SQMS) was used in kinetic uptake measurements and line-of-sight TPD measurements.[10] The shield was equipped with a rack-and-pinion driven sliding door that could, when open, expose the QMS ionization source to the random background of gas within the UHV chamber. Thus, the QMS can sample the random flux of PH_3 that misses or that is not adsorbed by the Si crystal during a kinetic uptake measurement. For direct line-of-sight studies of desorbing species from the center of the Si(111) crystal, a 5.0 mm diameter axially-located entrance aperture is employed, and the sliding door is closed.

The size of the aperture was chosen to be small in comparison to typical crystal dimensions thus permitting TPD measurements from the crystal center without contributions from possible desorption signals from metal supports. This procedure also eliminates the influence of crystal temperature gradients (optical pyrometry has shown that temperature gradients across the crystal are <10 K at 1080 K for our mounting procedure, see below). The entrance aperture is electrically isolated and can be biased to avoid ESD effects on the crystal surface from electrons emitted by the QMS ionization source. The aperture bias voltage is -100 V.

To achieve a reproducible crystal-aperture distance, a small tungsten wire curl was spot welded on the aperture and the electrical continuity between the

crystal and the aperture was monitored as the crystal was brought close to the aperture. The curl was fashioned to touch only the extreme edge of the Si crystal. Once continuity is established, the crystal is retracted 0.1 mm to provide a reproducible crystal-aperture geometry. The crystal-aperture distance is typically 2 mm.

The aperture housing is conically shaped to promote the deflection of large angle, non-line-of-sight desorbing species which might originate from leads and metal supports, causing spurious signals during TPD measurements. This conical geometry is important for the elimination of multiple reflections of desorbing species between the aperture and the crystal surface, which could deliver such species to the aperture. The QMS shield is differentially pumped by the UHV chamber through three equally spaced 1.1 cm diameter holes on the rear circumference of the QMS shield.

D. ESD and LEED measurements

A digital LEED/Electron Stimulated Desorption Ion Angular Distribution (ESDIAD) instrument was used to make LEED and accurate ESD yield measurements. A more detailed view of the present apparatus is shown in Fig. 2. An electron gun (Comstock EG-401) modified with x-y deflection plates serves as the electron beam source for these measurements. For the ESD H^+ yield measurements reported here, the crystal is biased at +100 V to ensure that all of H^+ ions produced by ESD are collected.

For ESD measurements, an electron beam (300 eV, 10^{-8} A) is used to excite a 1 mm diameter spot on the crystal. The resulting ESD ions are intercepted by 3 concentric hemispherical grids in the retarding field analyzer (G_1-G_3, numbered in order from the crystal). The grids are biased at: $V_1=V_2=0$ V, $V_3=+70$ V. The positive ions then pass through two planar grids, G_4 ($V_4=0$ V) and G_5 ($V_5=-500$

V), and are collected on the multichannel plate (MCP)/anode assembly located just beyond G_5. A gain of ~10^5 over the input ion current is achieved in the MCP/anode assembly and the resulting signal is fed to a computerized data collection and manipulation system that has been described previously.[11,12]

The production of a low energy X-ray background and electronically excited neutral (meta-stable) species is well known in such measurements and the digital acquisition system permits rapid in-situ background subtraction to obtain the true ESD ion yield.[11,12,13] To obtain such background data, G_3 is biased at V_3=+150 V to retard any ions produced by the ESD process. Thus, only the X-ray background and possible metastable species are collected. This background typically accounts for ~50% of the collected signal in this study.

The ESDIAD of the adsorbed species was examined and was found to give complicated angular information about the H^+ ions produced. Because a simple interpretation of the ESDIAD results is not presently possible, we report only the background-subtracted ESD H^+ ion yield integrated over all directions as a measure of the ESD effects on the PH_x adsorbate.

For LEED measurements, a 100 eV electron beam is used with currents below $1x10^{-9}$ A. The grids are biased as follows: V_1=V_2=V_3=0 V, V_4=-82 V, and V_5=0 V. Sharp LEED patterns are readily observed from clean, prepared crystal surfaces with this instrument.

E. Controlled PH_3 dosing of the crystal

The chamber also contains a microcapillary array doser for the production of a partially collimated PH_3 beam. The details of the doser are described elsewhere.[14] The phosphine gas was purified by several freeze-pump-thaw cycles and was stored in a stainless steel cylinder. A mass spectrum of the PH_3 showed no impurities above 1%, other than molecular H_2 which does not adsorb on

Si(111). We believe that the H_2(g) is produced from the walls of the stainless steel storage cylinder and is rapidly pumped away during PH_3 purification, leaving only PH_3(g). The gas, initially transferred to an adjacent storage reservoir, is admitted to the chamber through a nominal 2μm diameter conductance-limiting orifice. Thus, changing the phosphine pressure in the reservoir permits accurate control of the PH_3 flux emanating from the doser. In the adsorption measurements described here, the (reservoir) pressure-normalized phosphine flux is $F(PH_3)=1.93\pm0.09\times10^{13}$ PH_3 molecules $Torr^{-1}$ s^{-1}. Typical reservoir pressures, measured with a Baratron capacitance manometer, are ~0.2 Torr in the kinetic uptake measurements reported herein. The calibration of the flux is described elsewhere.[15] Using the measured flux, the fraction of molecules intercepted by the crystal, and the known crystal area, accurate coverage measurements can be made.[10,15,16] The fraction of molecules intercepted by the crystal can be directly observed in kinetic uptake measurements[15], or calculated from known crystal-doser array geometry.[17,18]

This dosing technique permits the enhancement of the local PH_3 density near the doser to be ~30 times that in other parts of the chamber.[17] As a result, the chamber pressure remains at $P\sim1\times10^{-10}$ Torr during exposures, thus minimizing possible displacement effects from the walls, large gas loads on pumps, etc. typically found in "system dosing" arrangements.

The dosing arrangement does not require the use of a BA ionization gauge (a source of ESD effects) and this gauge is therefore turned off during uptake measurements. However, the ESD e-gun and the shielded QMS filaments remain on and therefore the crystal is biased at -100 V during exposures to avoid any low-energy stray electrons from inducing ESD effects on the exposed surface.

F. Identification of positive ions produced by ESD

A second QMS, fitted with an electron gun identical to that employed in the LEED/ESD measurements, is used to identify the species produced from the ESD process. Typical electron beam currents received by the crystal surface during such measurements are ~$1x10^{-6}$ A. In this measurement, the internal filament in the QMS ionization source is turned off and the crystal and acceleration grids are biased so as to inject ESD-produced positive ions with 40 eV kinetic energy into the QMS. The ions are then mass filtered by the QMS and the ESD signal is digitally recorded. Both of the quadrupole mass spectrometers can be digitally mass-multiplexed and 1-6 masses/s can be acquired at a 8 kHz sampling rate.

Atomic hydrogen (deuterium), used in chemisorption and isotopic exchange studies[15], is produced from H_2 (D_2) gas (P~$1x10^{-8}$ Torr) using a tungsten spiral filament which operates at 1800 K. As in the phosphine dosing method previously described, a bias of -100 V is placed on the crystal to prevent ESD effects during exposures.

G. Crystal preparation

The Si(111) crystals used in this study were 13.03x13.09x1.5 mm, Czochralski grown, p-type, B doped (nominal resistivity=10 Ω-cm) single crystals oriented to within 1°. The crystal edges were slotted for mounting as described previously.[14] Prior to mounting and installation in UHV, the crystals were treated with the well known hydrogen peroxide-based immersion cleaning procedure for Si to remove residual organics and transition metals left from cutting.[19-21]

Final preparation in UHV was accomplished by Ar^+ ion bombardment at glancing incidence (2000 eV, ~$2x10^{-6}$ A) for ~15 min, and subsequent annealing at 1173 K for 5-10 minutes. The annealing was accomplished by resistive heating of

the crystal with a programmable temperature controller described elsewhere.[22] The temperature of the crystal was monitored by a chromel-constantan (Type-E) thermocouple inserted in a small Ta foil envelope which is spring-loaded into one of the slots.[14] The crystal was then slowly cooled (<5K/s) to ~ 120 K. This preparation procedure resulted in a sharp (7x7) LEED pattern. AES measurements of the clean, prepared surface are shown in Fig. 3. Using the established elemental sensitivities for AES[23], we estimate, on the basis of the signal-to-noise ratio, a lower limit of detectability (atomic fraction in depth of Auger sampling) for the following elements: [P]=0.01; [C]=0.02; [N]=0.01; [O]=0.01; and [Ni]=0.02. None of these elements were actually detected on our clean crystals.

III. RESULTS

A. Adsorption kinetics of PH_3 on Si(111)-(7x7)

The adsorption kinetics of PH_3 on Si(111)-(7x7) at 121 K, as monitored by the SQMS (door open), are shown in Fig. 4. A background signal is established with the clean, prepared Si(111) crystal rotated away from the doser. The UHV chamber pressure is typically $3x10^{-11}$ Torr during this time period. For the typical experiment shown in Fig. 4, at t=113 s, PH_3 is admitted to the chamber ("doser on") through the conductance-limiting orifice separating the PH_3 storage reservoir and the UHV chamber. The PH_3 partial pressure in the reservoir is 0.214 Torr during the uptake measurement shown.

During the period 113 s<t<316 s, the PH_3 partial pressure in the UHV chamber approaches a constant value ($\Delta P = \Delta_1+\Delta_2$ in Fig. 4.). The uncorrected BA

ionization gauge pressure during this period increases to ~1×10^{-10} Torr. AES analysis of the clean, prepared crystal following exposure to the background pressure of PH_3 during this period shows no evidence of P contamination of the crystal surface.

At t=316 s, the crystal is rotated into the PH_3 beam produced by the doser array and a drop in the PH_3 partial pressure is observed, denoted by Δ_1 in Fig. 4. The ratio $(\Delta_1)/(\Delta_1+\Delta_2)$ is a direct measure of the fraction of the available PH_3 flux intercepted by the crystal. This measurement of the intercepted fraction, $f=(\Delta_1)/(\Delta_1+\Delta_2)$, assumes that there are no multiple reflections of PH_3 between the doser and the crystal surface (i.e. the initial sticking coefficient So ≈ 1) and depends on the crystal-doser geometry. Using 14 separate kinetic uptake experiments, we find that the measured fraction of PH_3 molecules intercepted is $f_{exp.}=0.64 \pm 0.07$.[15]

A theoretical estimate of the intercepted fraction, f, was made, based on known crystal-doser geometry (crystal-doser distance = 0.5 cm), assuming a unity initial sticking coefficient, $S_0=1$.[15] We obtain a value of $f_{calc.}=0.70$. The excellent agreement between the measured and the calculated value suggests that an initial sticking coefficient of unity is reasonable. The observed initial uptake is expected to depend solely on crystal-doser geometry if $S_0=1$.[24]

The rate of adsorption remains constant until t=415 s, which corresponds to a PH_3 exposure of 1.6×10^{14} PH_3 cm^{-2}. Eleven separate adsorption experiments gave an average exposure in this constant uptake regime of $1.5 \pm 0.2 \times 10^{14}$ PH_3 cm^{-2}. A constant rate of adsorption with unity efficiency suggests a mobile (extrinsic) precursor mechanism is involved in PH_3 adsorption on Si(111)-(7x7).

After the region of constant uptake, a decreasing rate of adsorption is observed for t>415 s. This indicates that the PH_3 adsorption process is less efficient in this regime. From AES measurements, roughly 25-30% additional

uptake occurs until saturation of the $PH_x(a)$ species is observed.[15]

At t=1512 s, the crystal is rotated away from the doser, and a desorption "spike" signal caused by the mechanical rotation of the crystal support is seen. Finally, at t=1756 s, the PH_3 in the storage reservoir is pumped away and the initial background signal (and the original UHV base pressure) is reestablished.

Phosphine uptake is also confirmed by the detection of the P(LVV) Auger signal, as shown for a typical saturation exposure in Fig. 5 (right side).

It should be noted that the adsorption of PH_3 on Si(111)-(7x7) can be blocked by atomic hydrogen (deuterium) prior to PH_3 exposure, indicating that the surface dangling-bonds are the active sites.[15]

B. Thermal desorption studies

Temperature programmed desorption of PH_3 on Si(111)-(7x7) reveals that two reaction pathways are possible for the adsorbed species. Figure 6 shows all of the desorbing species observed from PH_3 adsorbed on Si(111)-(7x7) at 110 K. The heating rate for all TPD measurements reported here is dT/dt=1.6 K/s.

The center TPD spectrum shows that a molecularly adsorbed PH_3 species desorbs from the PH_3-saturated Si(111) surface. The yield of $PH_3(g)$ compared to the $H_2(g)$ yield is very small, suggesting that only a small fraction of a monolayer of PH_3 desorbs as $PH_3(g)$. A maximum desorption rate of PH_3 is observed at ~180 K, followed by additional PH_3 desorption processes up to ~550 K. Isotope mixing experiments, not shown here, rule out a recombinative process $(PH_x(a)+(3-x)H(a))$ leading to PH_3 desorption.[15] This molecular desorption yield from the bound molecular state(s) increases monotonically with PH_3 exposure until saturation at a PH_3 exposure of about 3.5×10^{15} PH_3 cm^{-2} is observed, as may be inferred from the behavior of the area of the desorption traces in Fig. 7. It should be noted that the initial filling of the PH_3 state(s) which

desorb as PH_3 is first observed only at PH_3 exposures above 1.5×10^{14} PH_3/cm^2. This is the exposure (coverage) in Fig. 4 where the process of efficient PH_3 adsorption (S=1) is terminated and a less efficient adsorption process occurs beyond this point (S<1).

The other reaction channel for the adsorbed species is the thermal decomposition of the $PH_3(a)$ and the subsequent desorption of $H_2(g)$ at T_{max}~740 K and $P_2(g)$ at T_{max}~1010 K. The observation of $H_2(g)$ and $P_2(g)$ clearly indicates that decomposition has taken place. No other desorbing species were observed in a thorough search which included possible reaction products such as: SiH_4 (and its associated mass spectrometer ionization fragments SiH^+ and SiH_2^+), fragments of Si_2H_6 ($Si_2H_5^+$), SiP, P_2H_4 and P_4. The identification of $P_2(g)$ as the desorbing species responsible for the depletion of P(a), instead of the $P_4(g)$, was carefully made and is reported elsewhere.[15]

The temperature dependence of the phosphorus concentration as measured by Auger spectroscopy is shown in Fig. 8. These measurements were made following an exposure of $\epsilon_{PH_3}=7.8\times10^{14}$ cm^{-2} at 120 K. The atomic fraction of P in the Auger sampling depth was obtained using known AES sensitivities[23] without electron escape depth corrections (which are expected to be similar for Si(LVV,92 eV) and P(LVV,120 eV) Auger electrons and thus to cancel out). To make these measurements, the crystal was heated to a given temperature and permitted to cool to ~120 K before AES measurements were made.

For temperatures between 120 K≤T≤300 K, the P concentration remains constant. The measurements do not reflect a decrease in P concentration due to the desorption of molecular $PH_3(a)$ (see Figs. 6 and 7). We believe that the Auger electron beam desorbs the molecular PH_3 rapidly. Therefore Auger spectroscopy measures only the strongly bound $PH_x(a)(x\leq3)$ species.

Heating the crystal between 300 K and 700 K results in a slight increase in

the apparent P concentration. The inset of Fig. 8 shows that, upon heating, the P(LVV) lineshape changes in a way which increases the peak-to-peak height, comparing spectrum A to spectrum B. This is related to a chemical effect presumably due to the breaking of P-H bonds and to a change in the bonding of P to Si in this temperature regime.

The P concentration remains constant for 700 K<T<900 K until $P_2(g)$ desorption is observed (T_{max}~1010K). This desorption rate maximum for $P_2(g)$ agrees well with the mid point in the decline of the P-Auger intensity at ~ 1025 K in Fig. 8.

The $H_2(g)$ desorption process observed at T~740 K (Fig. 6) is quite similar to that observed when atomic hydrogen is adsorbed on Si(111) in the well-known monohydride phase.[25] This indicates that Si-H bond formation has occurred from the $PH_3(a)$ thermal decomposition. To confirm this, the leading edge of the Si(LVV) AES feature was carefully monitored in a series of heating experiments where $PH_3(a)$ first decomposes and H_2 then desorbs. It is well-known that the bulk plasmon loss feature 17 eV below the main Si(LVV) AES feature, shown in Fig. 5, is sensitive to the presence of Si-H bonding.[26-29] As described previously by Bozack et al.,[28] we define the intensity of the plasmon loss feature ("A" in Fig. 5) and use the Si(LVV) feature ("B" in Fig. 5) to provide an "A/B ratio" which serves as a sensitive indication of the presence of Si-H species.

Figure 9 shows the behavior of this A/B ratio as a function of substrate temperature. Here the horizontal dashed line indicates the A/B ratio for clean Si(111). After adsorption of PH_3 (ϵ_{PH_3} = 7.8×10^{14} cm^{-2}) at T~120 K, a slight increase in the ratio is observed above that observed for the clean, prepared Si(111) surface. This suggests that some PH_3 dissociative adsorption is occurring at 120 K, although the error bar of this measurement makes this

observation tentative. Further heating, however, clearly indicates a gradual formation of a surface Si-H species as P-H bonds break, even below 300K. This A/B ratio is insensitive to the presence of adsorbed phosphorus, as shown by the constant value of the ratio (Fig. 9) during P_2(g) desorption (900 K<T<1200 K, Fig. 6). The increase in the A/B ratio between 120 K and 700 K is therefore attributed to the breaking of P-H bonds in chemisorbed PH_x(a) ($x \leq 3$) species to form Si-H bonds. Further heating beyond 700 K results in H_2(g) desorption (cf. Fig. 6) and the A/B ratio returns to that of a clean, prepared Si(111) surface.

It should also be noted that the removal of surface hydrogen by H_2(g) desorption permits additional PH_3 adsorption, confirming that active sites (dangling bonds) for PH_3 adsorption are produced when Si-H bonds break.[15]

C. Electron stimulated desorption measurements

ESD measurements at various electron kinetic energies of both the clean and PH_3-exposed ($\epsilon_{PH_3} = 1.2 \times 10^{14}$ cm^{-2}) Si(111) surface are shown in Fig. 10 using the QMS detector. Only H^+ and F^+ ions were detected in each case, and the F^+ signal is near the noise limit for these measurements.

From the data of Fig. 10, it is evident that even a "clean, prepared" silicon surface can have hydrogen terminating some (small) fraction of the dangling bond sites. The source of the H^+ is believed to originate from the bulk, and is described in more detail elsewhere.[30]

Based on the data in the lower panel of Fig. 10, we have chosen an incident electron energy of 320 eV in order to maximize the H^+/F^+(noise) ratio. In general, the generated ESD signals were found to decrease less than 10% over the course of a typical measurement (~1 min.) with the QMS detector.

The ESD H^+ yield was also measured, using the hemispherical LEED/ESDIAD

apparatus (Fig. 2), as a function of temperature for a surface initially exposed to PH_3 (exposure = 2.8×10^{15} PH_3 cm^{-2}). This measurement is shown in Fig. 11, where the total H^+ yield for a typical clean, prepared surface is shown as an open circle. The absolute value of this yield varies by as much a 50% and may have been sample-preparation dependent, (see below). The H^+ ESD yield from PH_3 adsorbed on Si(111) is shown in Fig. 11 as solid circles, and a precipitous drop in the ESD H^+ yield is observed for T above 400 K and below 650 K.

The H^+ ESD yield for a PH_3-saturated Si(111) crystal remains essentially constant from 120 K - 400 K as shown in Fig. 11. In this same temperature interval, approximately 90% of the molecular PH_3 thermal desorption occurs (Fig. 7). On this basis, we postulate that the H^+ ESD signal does not originate from adsorbed PH_3 species which can thermally desorb as $PH_3(g)$. The large drop in H^+ ESD yield occurs in the temperature interval 400 - 650 K, prior to H_2 desorption from Si-H species. Thus the H^+ ESD yield is not due primarily to Si-H surface species. We therefore attribute the majority of the H^+ ESD yield to PH_x species ($3 \geq x \geq 1$) which form even at 120 K and which do not thermally desorb as $PH_3(g)$. As extensive P-H bond scission occurs above 300 - 400 K, the H^+ ESD yield decreases. This drop in H^+ ESD yield corresponds roughly to the temperature range where the P-Auger lineshape (Fig. 8) changes (300 - 600 K) and where Si-H bond formation is observed to occur from changes in the Si(LVV) Auger lineshape (120 - 500 K) (Fig. 9). However, there seems to be no exact correlation of the H^+ ESD yield with other measurements which have been made. It is also evident that the H^+ yield is sensitive to sample preparation, since the H^+ ESD yield after heating the PH_3-exposed crystal to 1150 K followed by cooling is lower than the yield obtained by the standard UHV preparation (Ar^+ ion bombardment, 1173 K anneal, 5-10 min) of a clean crystal as described above. Studies of this H^+ ESD yield from clean, prepared Si(111), believed to be due to bulk H

diffusion to the surface, will be reported elsewhere.[30]

IV. DISCUSSION

A. Adsorption processes

The kinetic uptake measurements of Fig. 4 clearly indicate that two types of adsorption processes occur for PH_3 adsorption on Si(111)-(7x7) at 120 K.

The first process (at constant sticking probability where $S_0 \approx 1$, Fig. 4) occurs over a range of coverage achieved up to a PH_3 exposure of ϵ_{PH_3} = $1.5 \pm 0.2 \times 10^{14}$ PH_3 cm^{-2}. The observed constant rate of adsorption in this regime clearly indicates that an extrinsic mobile precursor adsorption mechanism is being observed at 120 K.[31] Furthermore, the lifetime in the precursor state is long enough to permit substantial sampling of surface sites until PH_3 acommodation on the surface occurs. The observation of a unity sticking coefficient is in agreement with previous studies of PH_3 adsorption on Si(100).[6,8]

The second adsorption process, (t>415 s, Fig. 4), results in an additional PH_3 uptake of 20-25%, based on AES measurements.[15] This indicates that the saturation coverage of PH_x-producing PH_3 species on Si(111) corresponds to a PH_3 coverage of approximately $1.9 \pm 0.3 \times 10^{14}$ PH_3 cm^{-2} at 120 K. In this higher coverage regime, above 1.5×10^{14} PH_3/cm^2, the lifetime of the PH_3 precursor species begins to limit the ability of a molecule to find a chemisorption site before desorption of the precursor occurs. Thus the adsorption probability falls below unity, S<1, and the adsorption process is less efficient. PH_3(a) species are apparently stabilized at higher surface coverages, and become evident in TPD above a PH_3 exposure of 1.5×10^{14} PH_3/cm^2. A similar sequence of two adsorption processes has been observed for NH_3 on Si(100), where a unity

sticking coefficient process was followed by a process involving less efficient capture of NH_3 by the surface at 120 K.[32]

B. Estimate of PH_3 saturation coverage on Si(111)-(7x7)

A crude comparison of the saturation coverage of the PH_x-producing PH_3 species to the dangling bond (d-b) density can be made, based on the known density for the (7x7) unit cell of Si(111). One assumes in this estimate that all 19 d-b participate in the adsorption of PH_3 on Si(111)-(7x7). It should be noted, however, that d-b, site specific reactivity has been reported for NH_3 adsorption on Si(111)-(7x7).[33] Without such information for phosphine, we tentatively assume that all 19 d-b can participate in the reaction process. This corresponds to a d-b surface density of 3.0×10^{14} Si d-b cm^{-2}.

Thus, with a d-b density of 3.0×10^{14} Si d-b cm^{-2} in the (7x7) unit cell, the ratio of the PH_x-producing PH_3 species ($1.9 \pm 0.3 \times 10^{14}$ cm^{-2}) to the d-b density is $\theta_{PH_3,sat} \approx 0.5$-$0.7$ PH_3/Si d-b. This coverage suggests that steric hindrance, dangling-bond site-specificity, or dissociative adsorption to block further PH_3 adsorption may be responsible for the estimated saturation coverage. Saturation coverages for PH_3 which are less than unity under similar conditions have been reported by others on Si(100)[7,8] and Si(111)[5,9].

Simple packing arrangements of PH_3 molecules having the van der Waals diameter in the (7x7) unit cell lead to saturation coverages greater than unity. Thus, steric arguments limiting $\theta_{PH_3,sat}$ are not favored.[15]

Specific dangling-bond site chemistry has been observed in the case of NH_3 adsorption on Si(111)-(7x7).[33] In that work, Wolkow and Avouris observed that Si rest-atom sites were more reactive to NH_3 than "center" and "corner" ad-atom sites, with "center" ad-atoms more reactive than "corner" ad-atoms. This would lead to ~15 d-b sites when saturation coverages of NH_3 are involved. Assuming

that these 15 dangling-bonds could participate in the reaction of PH_3 with Si(111)-(7x7), a d-b density of 2.4×10^{14} Si d-b cm^{-2} would exist. Thus on this revised estimate of the density of reactive d-b sites, saturation coverages of PH_3 could be $\theta_{PH_3,sat} \approx 0.7\text{-}0.9$ PH_3/d-b, still less than the stoichiometric ratio, 1 PH_3/d-b.

Thus we are led to a supposition that all d-b sites are not available to PH_3 molecules. There are two possible explanations for this observation: (1) The dangling bond sites, by virtue of their differing electronic character, are not equally able to bond PH_3, or (2) Partial dissociation of $PH_3(a)$ to produce $PH_x(a) + H(a)$ results in blockage of the available d-b sites from full occupancy by PH_3 at saturation at 300 K.

C. Thermal Decomposition of $PH_3(a)$ and $PH_x(a)$ Species

It is possible that adsorption of PH_3 at 120 K on Si(111) is accompanied by partial dissociation of some $PH_3(a)$ species producing $PH_x(a) + H(a)$. Additional $PH_3(a) + PH_x(a)$ decomposition occurs in the temperature range ~ 120 - 600 K, based on three separate observations in this work as listed below:

(1) Evidence for P-H bond scission to produce Si-H bonds is found in AES studies of the Si(LVV) spectrum, Fig. 5, and the behavior of the "A/B" ratio on heating (Fig. 9). The "A/B" ratio increases over the temperature range 120 K - 500 K, then decreases as H_2 is desorbed above ~ 700 K.

(2) Additional evidence for loss of P-H bonds above ~ 400 K is seen by the loss of H^+ ESD yield. The decrease in H^+ yield corresponds to the decomposition of $PH_3 + PH_x$ species (Fig. 11).

(3) A subtle change in the P(LVV) Auger lineshape in the 300 - 600 K range

(Fig. 8) is also indicative of P-H bond scission in this temperature region.

D. Thermal Desorption of $PH_3(a)$, $H_2(g)$ and $P_2(g)$

It is evident that molecular PH_3 may be bonded to Si(111)-(7x7), and that this occurs with the formation of fairly strong Si-P bonds. These PH_3 species are not observed by TPD at coverages below ~ 1.5×10^{14} PH_3 cm^{-2}. A wide range of Si-PH_3 binding energies are possible, given that the desorption temperature for $PH_3(g)$ occurs over the range 120 K - ~ 550 K. The thermal desorption of PH_3 is not due to a surface recombination process, since isotopic mixing experiments involving D(a) do not yield deuterated phosphine species.[15] The thermal desorption of molecular PH_3 was also reported by Yu, et al.[8] at higher temperatures on Si(100).

H_2 desorption occurs above ~ 650 K, yielding characteristic monohydride desorption kinetics, without evidence for dihydride or SiH_4 production. Desorption of H_2 produces active sites capable of further PH_3 adsorption.[15]

P_2 desorption above ~ 910 K occurs without production of $P_4(g)$. The observation of P depletion through $P_2(g)$ desorption instead of extensive P depletion through diffusion into the bulk at these temperatures is in agreement with the diffusion coefficients measured in neutron activation analysis studies of P on Si(100).[34] Yu, et al.[8] also found P_2 production from PH_3 on Si(100).

E. Energetics of PH_3 Decomposition

Simple bond energy arguments suggest that P-H bond scission on Si(111) is thermodynamically favorable. Consider the process

$$PH_3(g) + Si(111) \rightarrow PH_2(a) + H(a) \quad (1)$$

$$\Delta H \cong -D°(Si\text{-}PH_2) - D°(Si\text{-}H) + D°(H_2P\text{-}H)$$

$$= -D°(Si\text{-}PH_2) - 90 \text{ kcal/mol}^{35} + 90.3 \text{ kcal/mol}^{36}$$

$$\cong -D°(Si\text{-}PH_2)$$

While we do not know the value of $D°(Si\text{-}PH_2)$, process (1) will be thermodynamically favorable. It is noted that $D°(Si\text{-}P) = 88$ kcal/mol[36].

V. SUMMARY

We observe that PH_3 adsorbs on Si(111)-(7x7) with an initial sticking coefficient of $S_0 \approx 1$ through an extrinsic mobile precursor mechanism at 120 K up to ~70-75% of saturation. AES measurements indicate that at 120 K some dissociative adsorption occurs. Coverage measurements indicate that if one assumes that all of the available 19 dangling bonds in the (7x7) unit cell react with phosphine, the saturation coverage of the PH_x-producing PH_3 species is ~ 0.5 - 0.7/d-b. PH_x surface species yield H^+ in ESD, and the decrease in H^+ yield may be used to follow P-H bond scission.

The thermal decomposition of the $PH_3(a) + PH_x(a)$ species is shown in Fig. 12, which serves to summarize our observations. In the temperature range of 120 K<T<550 K, $PH_3(g)$ is liberated and the $PH_3(a) + PH_x(a)$ species decompose to deliver H to free Si dangling bond sites forming Si-H species. Further heating to T>700 K results in the desorption of $H_2(g)$ (which provides dangling bond sites for further PH_3 adsorption). Heating to T>1000 K results in complete surface phosphorus depletion through $P_2(g)$ desorption. Upon annealing to 1200 K, the surface is rendered "clean" with some small concentration of surface Si-H species still present as observed by H^+ ESD.

VI. ACKNOWLEDGEMENTS

The full support of the Office of Naval Research is gratefully acknowledged. The authors would like to thank Ms. Shenda Baker for her assistance in the preliminary stages of the work.

REFERENCES

a) Department of Physics and Astronomy, University of Pittsburgh, Pittsburgh PA, 15260.

1 F.Shimura, Semiconductor Silicon Crystal Technology, (Academic Press, San Diego, Calif., 1989).

2 J.M.Jasinski, B.S.Meyerson, and B.A.Scott, Ann. Rev. Phys. Chem. 38, 109 (1987).

3 A.J.Van Bommel and F.Meyer, Surf. Sci. 8, 381 (1967).

4 J.J.Lander and J.Morrison, J. Chem. Phys. 37, 729 (1962).

5 A.J.Van Bommel and J.Crombeen, Surf. Sci. 36, 773 (1973).

6 B.S.Meyerson and M.L.Yu, J. Electrochem. Soc. 131, 2366 (1984).

7 B.S.Meyerson and M.L.Yu, J. Vac. Sci. Technol. A2, 446 (1984).

8 M.L.Yu, D.J.Vitkavage and B.S.Meyerson, J. Appl. Phys. 59, 4032 (1986).

9 A.H.Boonstra, Phillips Res. Rept. Suppl. no. 3, (1968).

10 An example of a shielded QMS of slightly different design can be found in: V.S.Smentkowski and J.T.Yates,Jr., J. Vac. Sci. Technol. A7, 3325 (1989).

11 M.J.Dresser, M.D.Alvey and J.T.Yates, Jr., Surf. Sci. 169, 91 (1986).

12 M.J.Dresser, M.D.Alvey and J.T.Yates, Jr., J. Vac. Sci. Technol. A4, 1446 (1986).

13 R.M.Wallace, M.J.Dresser, P.A.Taylor, J.T.Yates,Jr., to be published (1990).

14 M.J.Bozack, L.Muehlhoff, J.N.Russell, Jr., W.J.Choyke and J.T.Yates, Jr., J. Vac. Sci. Technol. A5, 1 (1987).

15 P.A.Taylor, R.M.Wallace, W.J.Choyke and J.T.Yates, Jr., submitted Surf. Sci., (1990).

16 C.C.Cheng, R.M.Wallace, P.A.Taylor, W.J.Choyke and J.T.Yates, Jr., accepted J. Appl. Phys., (1990).

[17] C.T.Campbell and S.M.Valone, J. Vac. Sci. Technol. A3, 408 (1985).

[18] A.Winkler and J.T.Yates, Jr., J. Vac. Sci. Technol. A6, 2929 (1988).

[19] W.Kern and D.A.Puotinen, RCA Rev. 31, 187 (1970).

[20] R.C.Henderson, J. Electrochem. Soc. 119, 772 (1972).

[21] A convenient summary of this procedure can be found in ref. 1, appendix XII.

[22] R.J.Muha, S.M.Gates, P.Basu and J.T.Yates, Jr., Rev. Sci. Instr. 56, 613 (1985).

[23] P.W.Palmberg, G.E.Riach, R.E.Weber and N.C.MacDonald, Handbook of Electron Spectroscopy, (Physical Electronics, Edina, MN, 1972).

[24] T.M.Madey, Surf. Sci. 33, 355 (1972).

[25] G.Schulze and M.Henzler, Surf. Sci. 124, 336 (1983).

[26] H.H.Madden, Surf. Sci. 105, 129 (1981).

[27] H.H.Madden, D.R.Jennison, M.M.Traum, G.Margaritondo and N.G.Stoffel, Phys. Rev. B26, 896 (1972).

[28] M.J.Bozack, P.A.Taylor, W.J.Choyke and J.T.Yates, Jr., Surf. Sci. 179, 132 (1987).

[29] J.Woicik, B.B.Pate and P.Pianetta, Phys. Rev. B39, 8593 (1989).

[30] R.M.Wallace, P.A.Taylor, W.J.Choyke and J.T.Yates, Jr., to be published.

[31] W.H.Weinberg, in: Kinetics of Interface Reactions, Eds. M.Grunze and H.J.Kreuzer, (Springer, New York, 1987) 94.

[32] M.J.Dresser, P.A.Taylor, R.M.Wallace, W.J.Choyke and J.T.Yates, Jr., Surf. Sci. 218, 75 (1989).

[33] R.Wolkow and Ph. Avouris, Phys. Rev. Lett. 60, 1049 (1988).

[34] J.S.Makris and B.J.Masters, J. Electrochem. Soc. 120, 1252 (1973).

[35] K.Sinniah, M.G.Sherman, L.B.Lewis, W.H.Weinberg, J.T.Yates, Jr. and K.C.Janda, Phys. Rev. Lett., 62, 567 (1989); also J. Chem. Phys., accepted.

[36] F.E.Saalfeld and H.J.Svec, Inorg. Chem. 3, 1442 (1964).

FIGURE CAPTIONS

Fig. 1. A schematic diagram of the UHV apparatus used in this study. Base pressure of the system is 3×10^{-11} Torr.

Fig. 2. A cross-sectional view of the digital LEED/ESDIAD apparatus used for LEED and H^+ ESD yield measurements.

Fig. 3. Typical dN(E)/dE Auger spectra of the clean Si(111) surface.

Fig. 4. Adsorption kinetics of phosphine on Si(111)-(7x7) at 121 K as monitored by the shielded QMS with the shield door open (see text). Two adsorption processes are observed: a fast $S_0=1$ process up to a coverage of 1.6×10^{14} PH_3 cm^{-2}, and a slower $S<1$ process in which molecular adsorption occurs.

Fig. 5. Definition of the "A/B ratio" employed to study the formation of Si-H species and a typical P(LVV) Auger signal.

Fig. 6. The desorption products observed by temperature programmed desorption from PH_3 adsorbed on Si(111)-(7x7). Comparison of the integrated area of the PH_3 to that of H_2 suggests that the observed $PH_3(g)$ corresponds only to a small fraction of a monolayer.

Fig. 7. Development of the molecular $PH_3(g)$ desorption state(s) with increasing PH_3 exposure. The molecular PH_3 desorption state(s) is observed only for high exposures of PH_3 and is initially filled in the $S<1$ region of Fig. 4.

Fig. 8. Apparent phosphorus concentration and P(LVV) lineshape for PH_3/Si(111) as a function of temperature (line drawn to guide the eye). The breaking of P-H bonds in the PH_x(a) species is observed as a chemical effect on the P(LVV) lineshape. The phosphine exposure for this experiment was $\epsilon_{PH_3} = 7.8 \times 10^{14}$ cm^{-2}.

Fig. 9. The formation of Si-H bonds as a function of temperature as determined from the "A/B ratio" in Fig. 5 (line drawn to guide the eye). The phosphine exposure in this experiment is $\epsilon_{PH_3} = 7.8 \times 10^{14}$ cm^{-2} (see Fig. 8).

Fig. 10. Electron stimulated desorption of H^+ ions from clean, prepared and PH_3-exposed Si(111). The F^+ ESD signal is near the noise limit for these measurements. The phosphine exposure in this experiment is $\epsilon_{PH_3} = 1.2 \times 10^{14}$ cm^{-2}.

Fig. 11. H^+ ESD yield from PH_x(a) as a function of temperature (line drawn to guide the eye). The phosphine exposure for this experiment is $\epsilon_{PH_3} = 2.8 \times 10^{15}$ cm^{-2}.

Fig. 12. Summary schematic of the adsorption and thermal decomposition of phosphine on Si(111)-(7x7).

Ultrahigh Vacuum Apparatus for Silicon Surface Chemistry

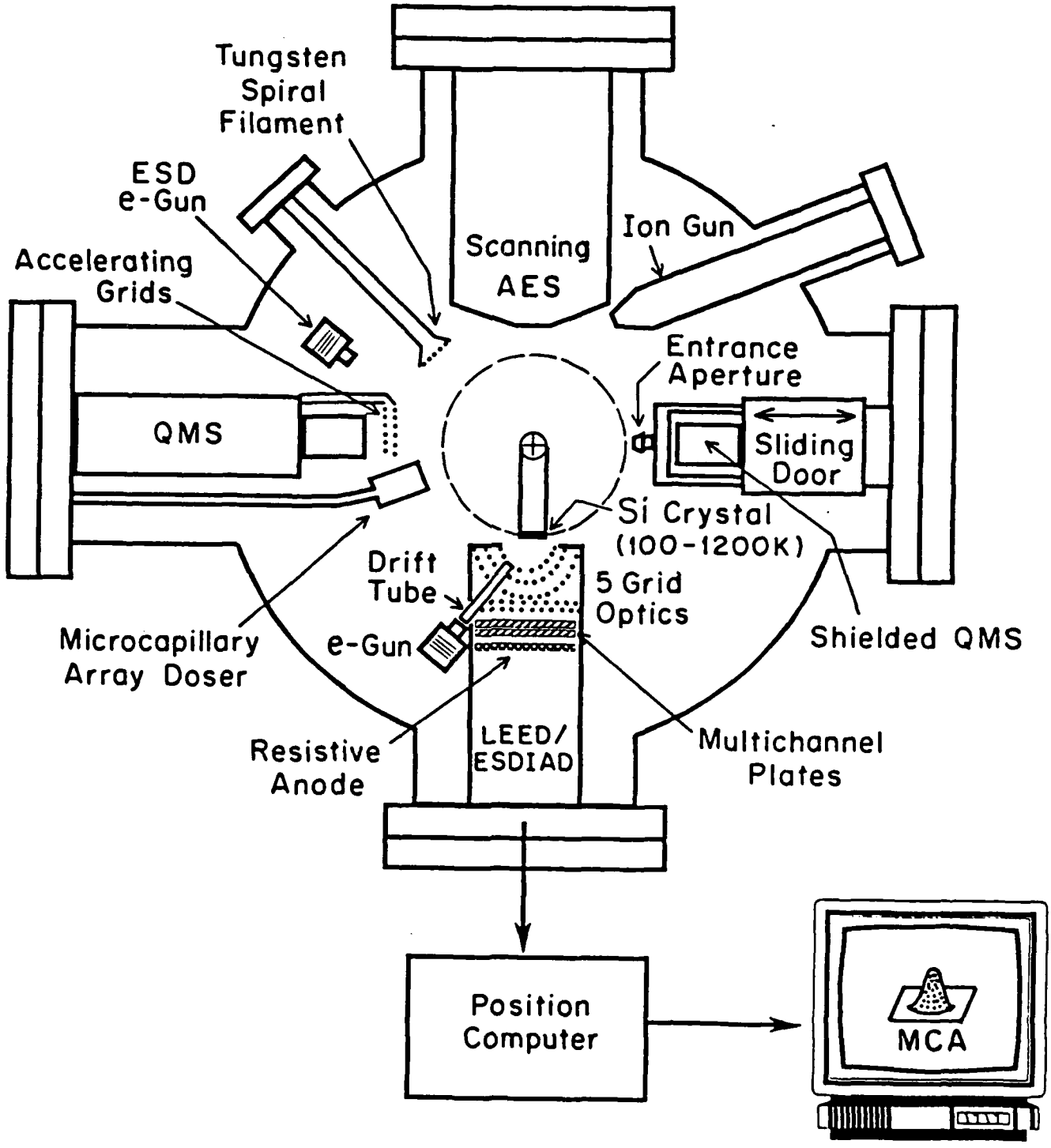

Wallace,
Taylor, Choyke
Yates
Figure 1

Cross-sectional View of Digital LEED/ESDIAD Apparatus

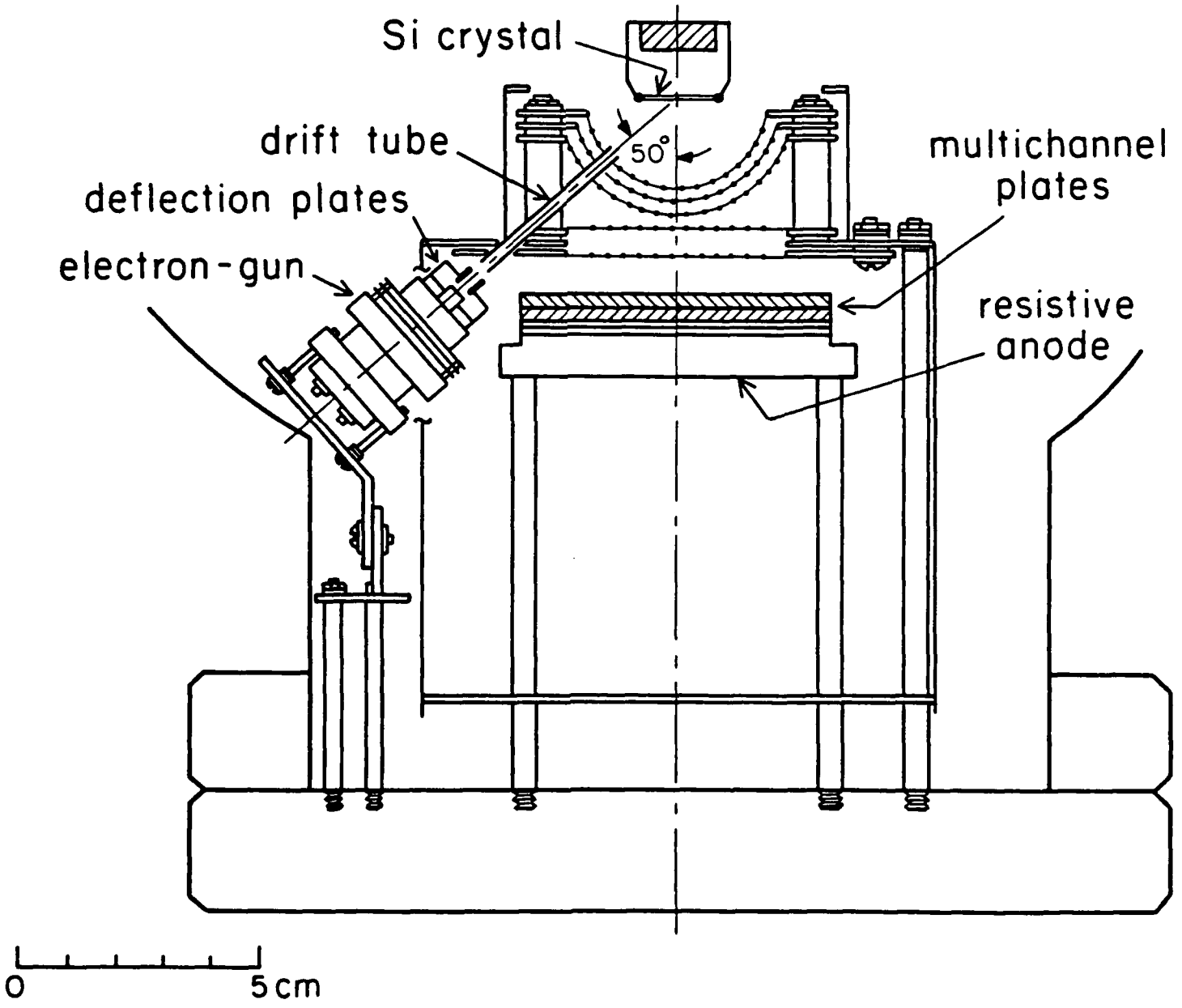

Wallace,
Taylor, Choyk
Yates
Figure 2

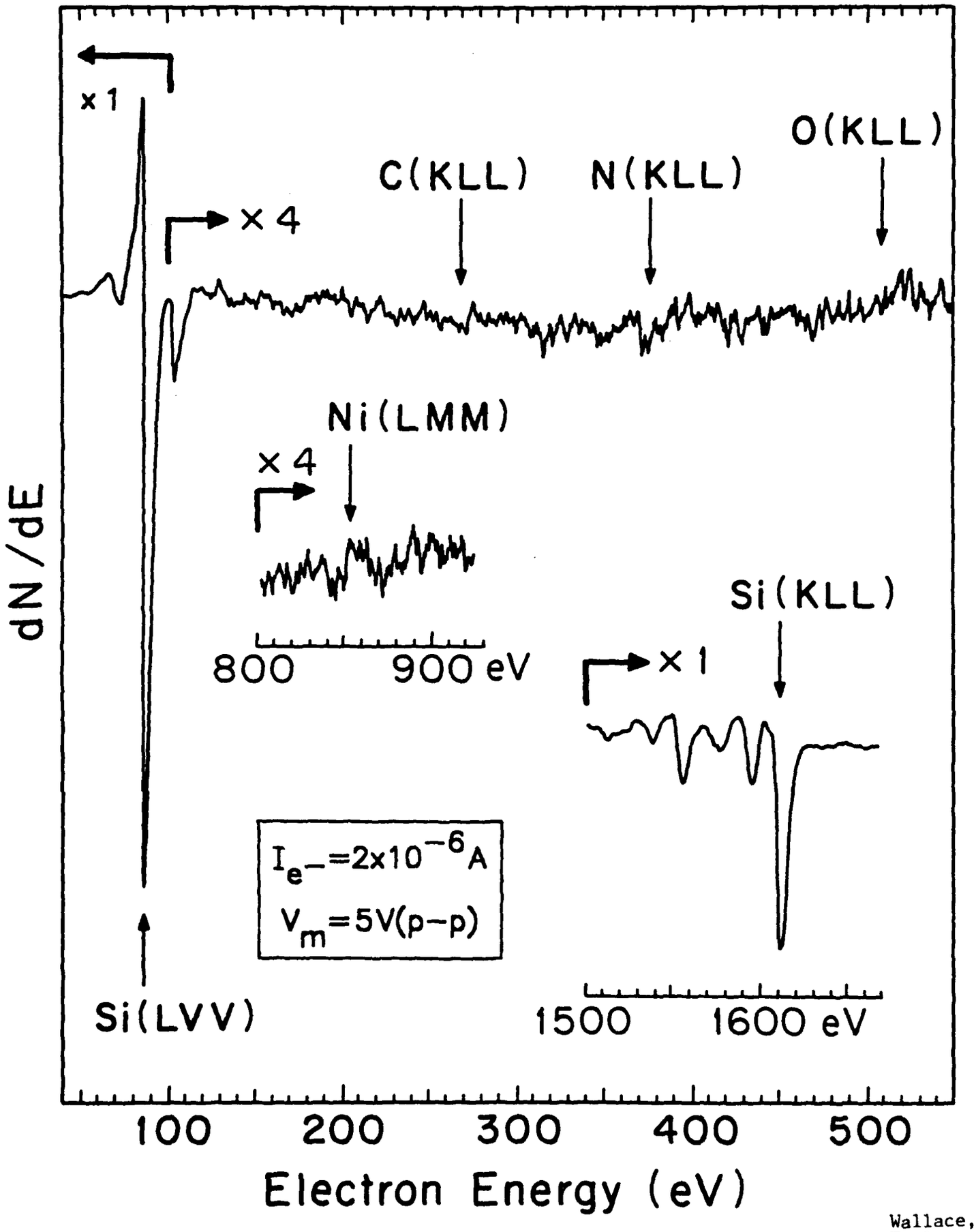

Wallace,
Taylor, Choy
Yates
Figure 3

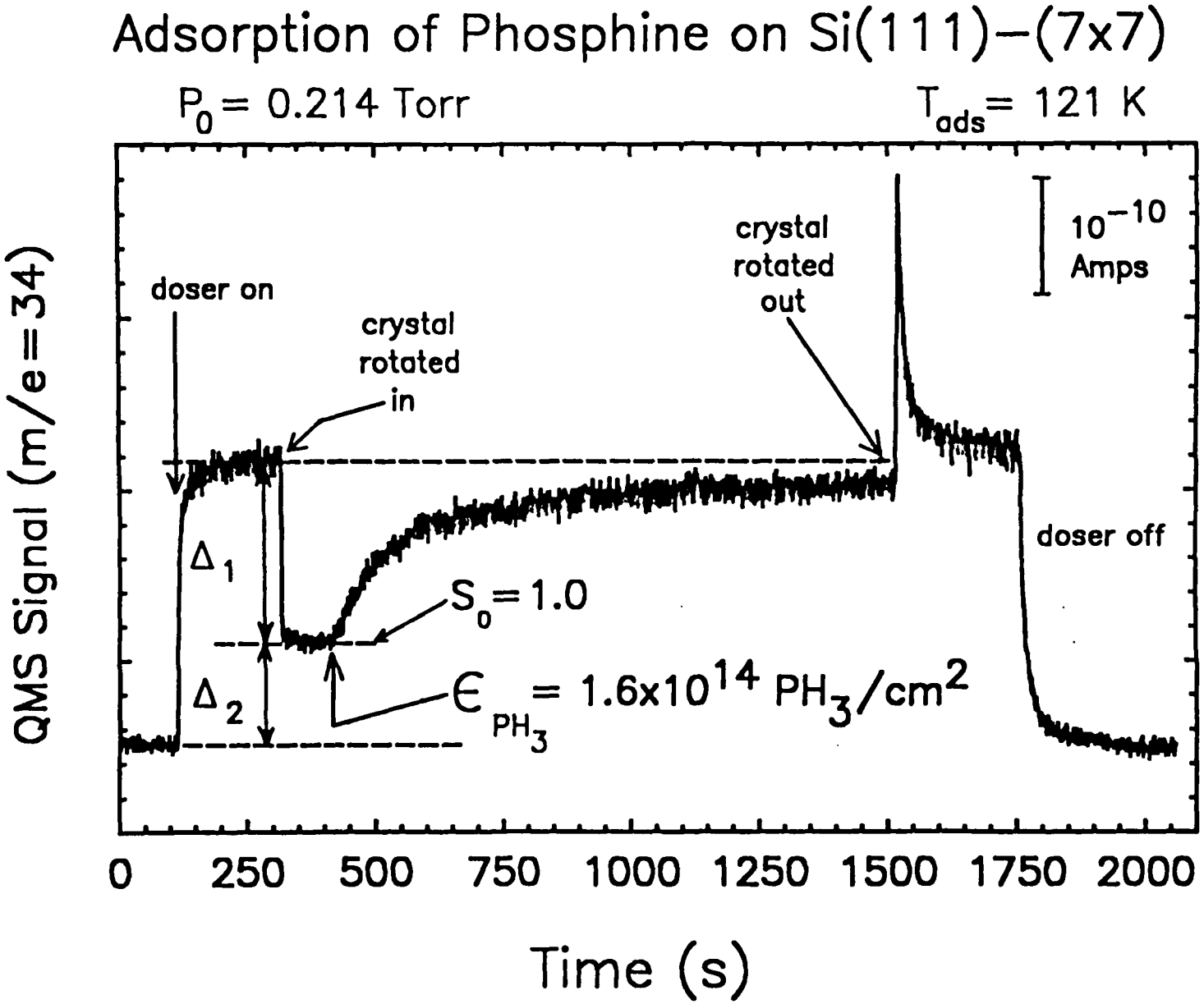
Adsorption of Phosphine on Si(111)–(7x7)
P_0 = 0.214 Torr
T_{ads} = 121 K
QMS Signal (m/e=34)
doser on
crystal rotated in
crystal rotated out
10^{-10} Amps
doser off
Δ_1
Δ_2
S_0 = 1.0
ϵ_{PH_3} = 1.6x10^{14} PH_3/cm^2
0
250
500
750
1000
1250
1500
1750
2000
Time (s)

AES Spectra following PH_3 Adsorption on Si(111) at 135 K

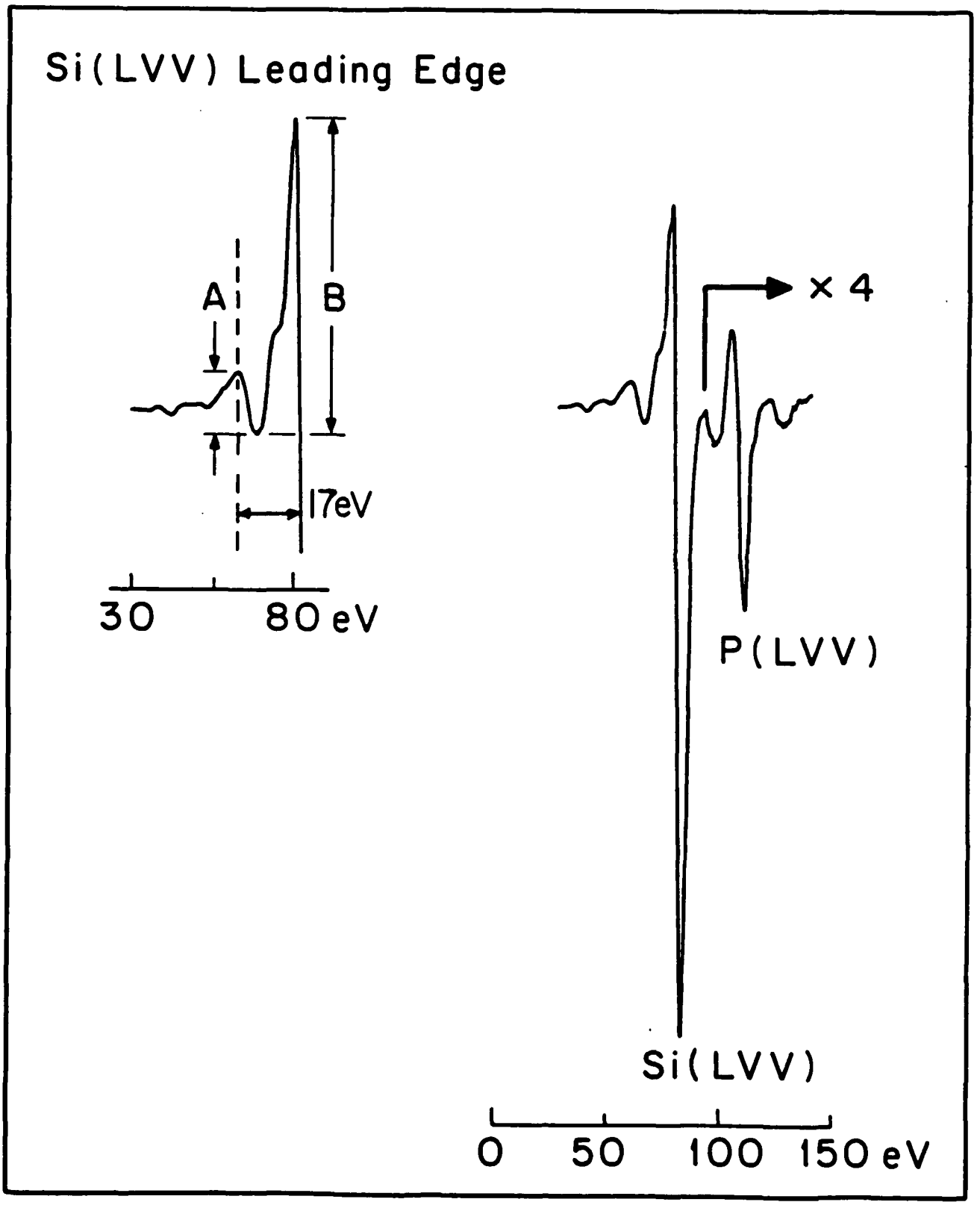

Wallace,
Taylor, Choyk
Yates
Figure 5

Thermal Desorption from $PH_3/Si(111)-(7x7)$

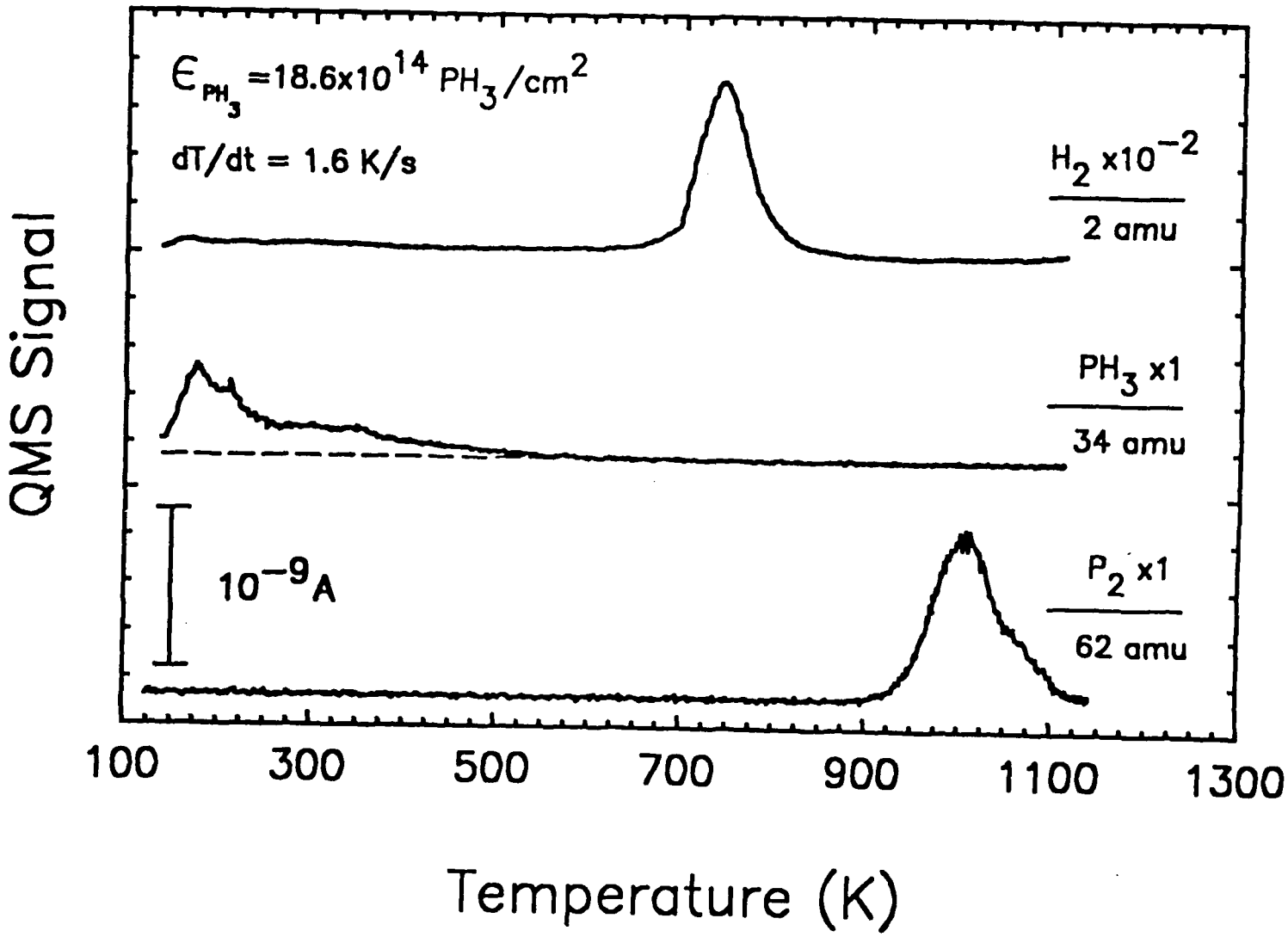

Thermal Desorption of PH_3 from PH_3/Si(111)

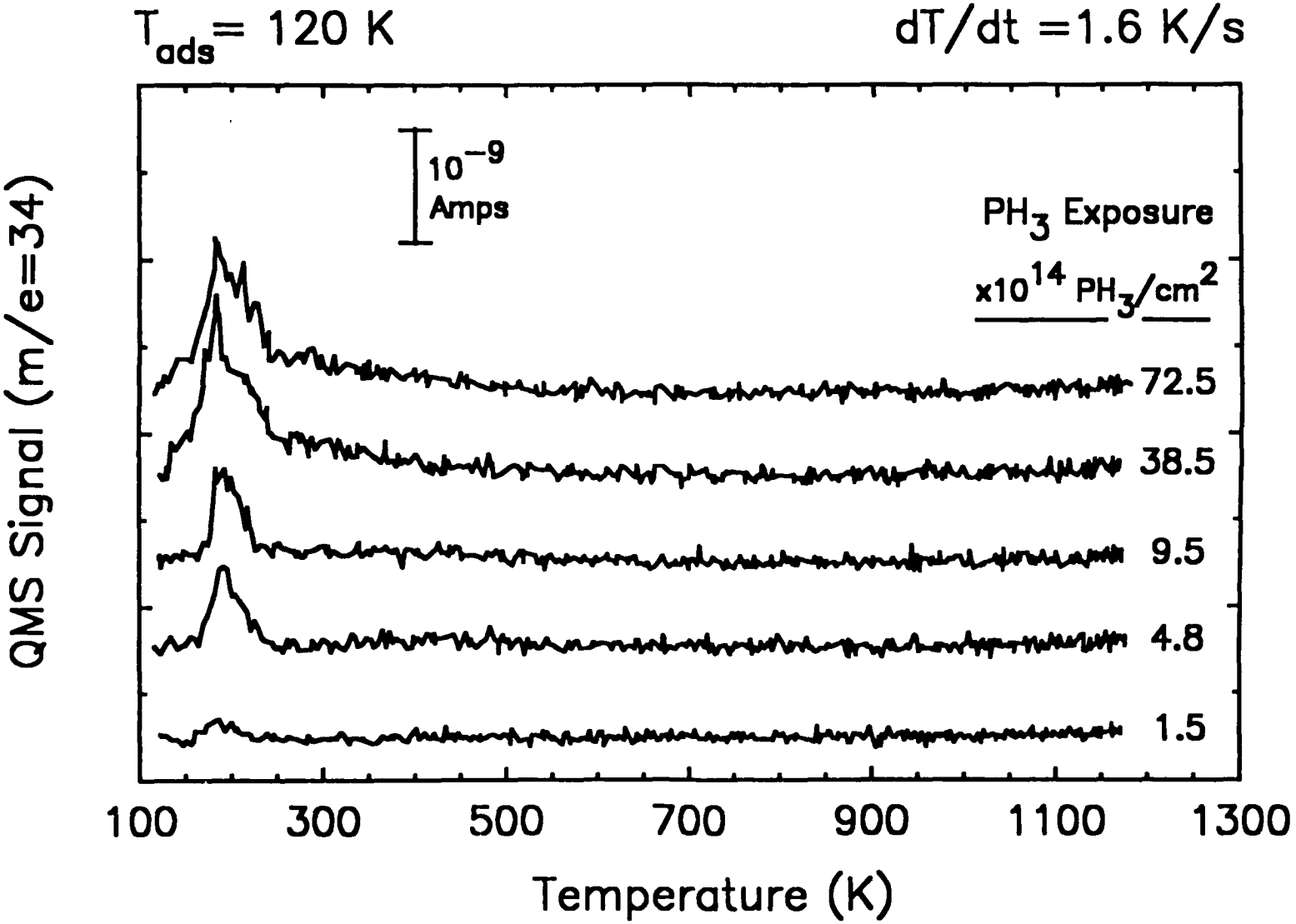

Wallace,
Taylor, Choyke
Yates
Figure 8

Wallace, Taylor, Choyke Yates
Figure 9

Behavior of Si(LVV) Auger Lineshape upon Annealing— PH_3 on Si(111)

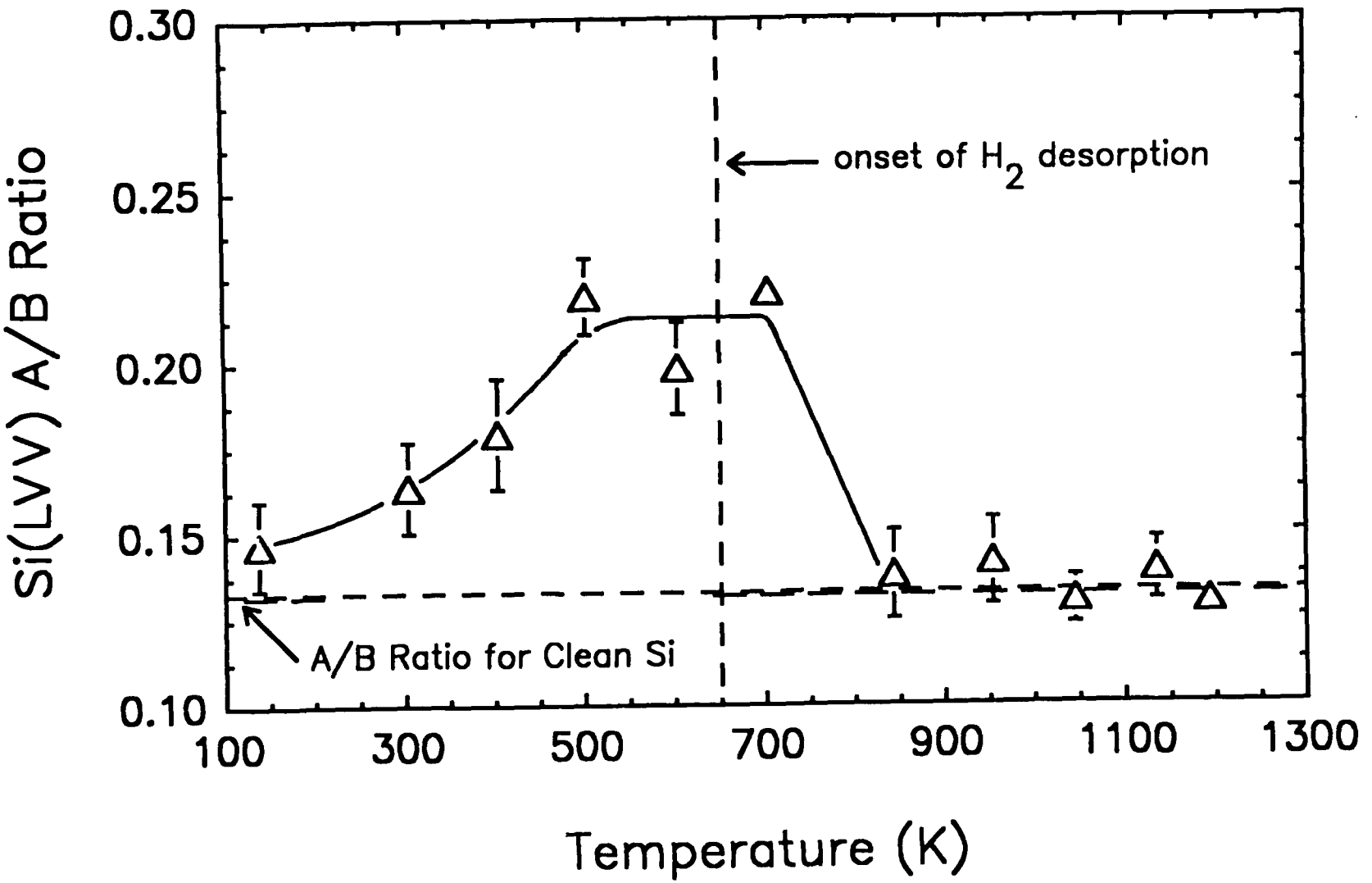

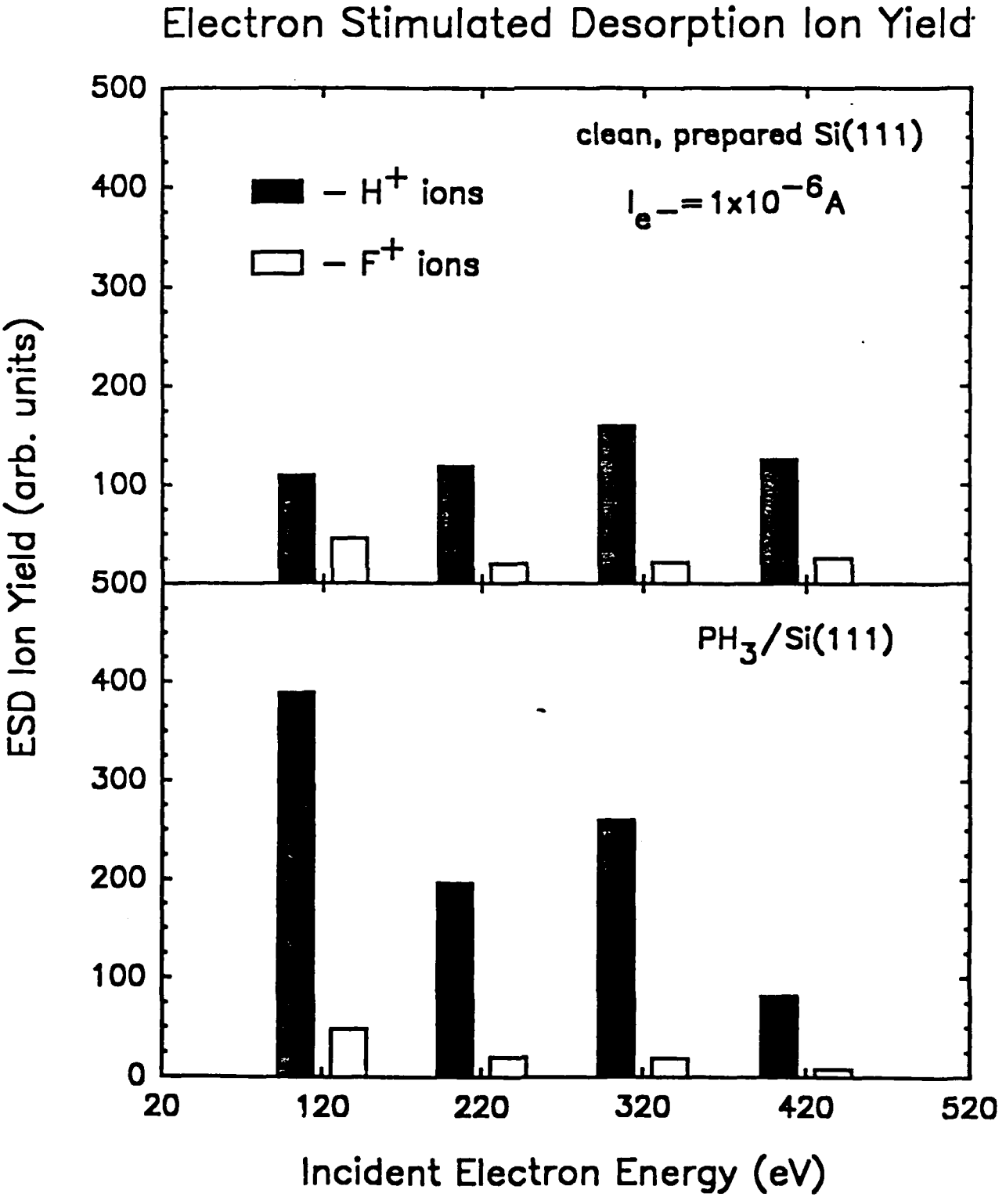

Wallace,
Taylor, Choy
Yates
Figure 10

Wallace,
Taylor, Choyke
Yates
Figure 11

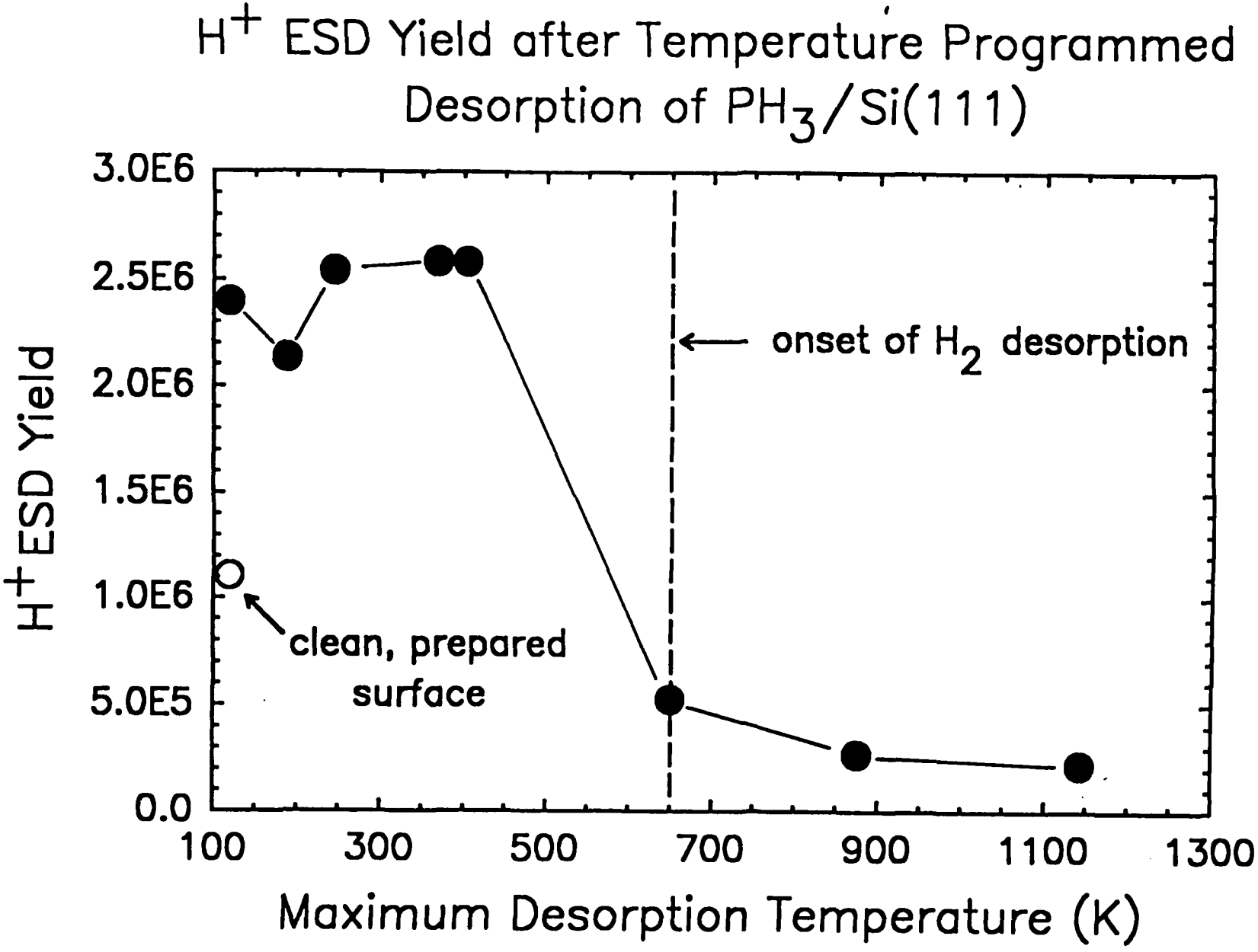

Schematic of the Thermal Decomposition of Phosphine on Si(111)-(7x7)

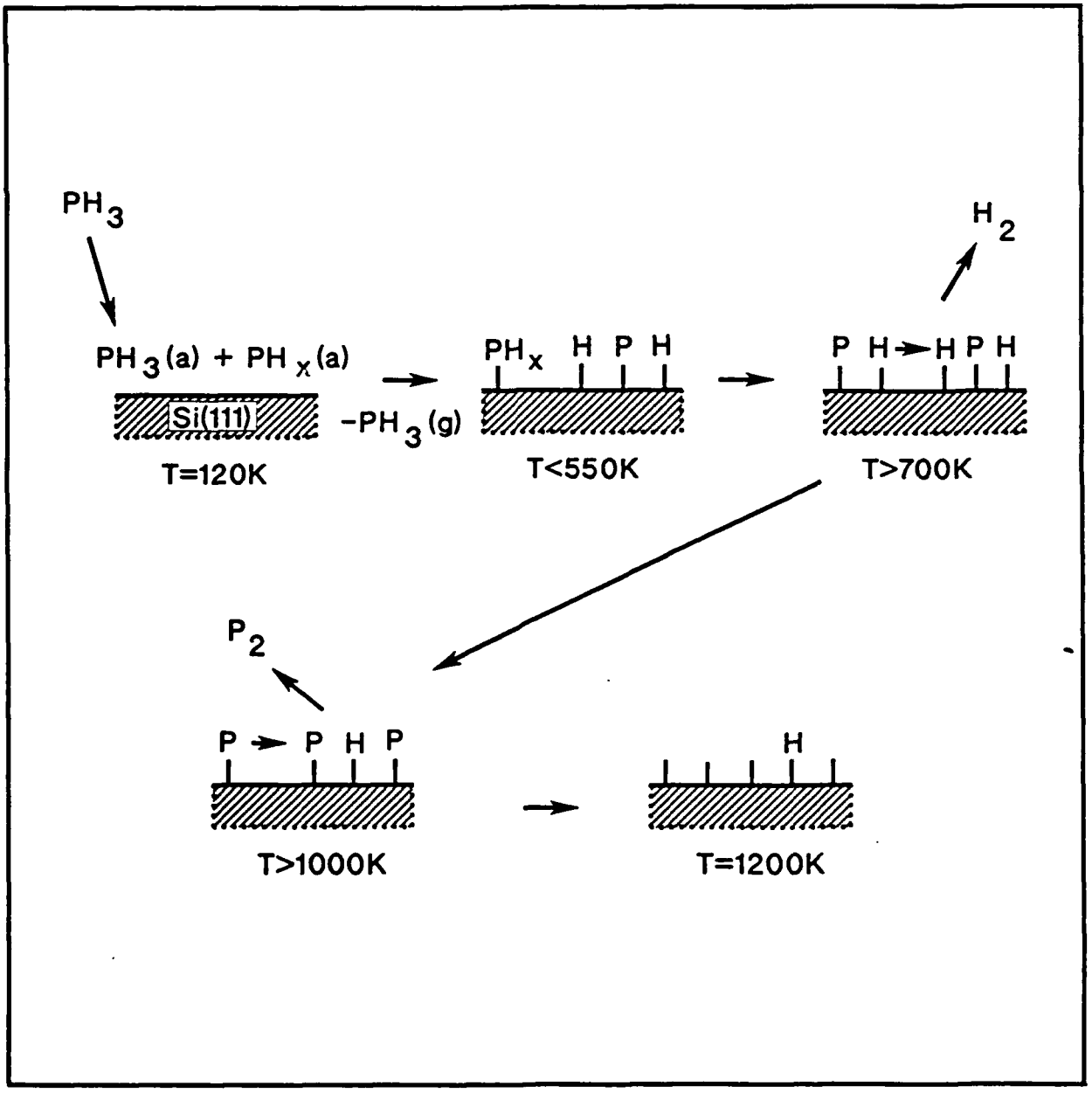

Wallace,
Taylor, Choyke,
Yates
Figure 12

TECHNICAL REPORT DISTRIBUTION LIST, GEN

	No. Copies
Office of Naval Research Attn: Code 1113 800 N. Quincy Street Arlington, VA 22211-5000	2
Dr. Bernard Douda Naval Weapons Support Ctr. Code 50-C Crane, IN 57522-5050	1
Naval Civil Engr. Lab. Attn: Dr. R.W. Drisko Code L-52 Port Hueneme, CA 92401	1
Defense Technical Information Center Bldg. 5, Cameron Station Alexandria, VA 22314	12
DTNSRDC Attn: Dr. H. Singerman Applied Chemistry Division Annapolis, MD 21401	1
Dr. William Torres, Supt. Chemistry Div., Code 6100 Naval Research Laboratory Washington, DC 20375-5000	1
Dr. Mark Ross ONR 800 N. Quincy Street Arlington, VA 22217-5000	3
Dr. David Young Code 334 NORDA NSTL, Miss 39429	1
Naval Weapons Ctr. Attn: Dr. Ron Atkins Chemistry Division China Lake, CA 93555	1
Scientific Advisor (WF06B) Marine Corp-Ground Task Force Warfighting Center Marine Corps Combat Development Command Quantico, VA 22134-5001	1
U.S. Army Research Office Attn: CRD-AA-IP PO Box 12211 Res. Triangle Park, NC 27709	1
Mr. John Boyle Materials Branch Naval Ship Engr. Ctr. Philadelphia, PA 19112	1
Naval Oceans Systems Ctr. Attn: Dr. S. Yamamoto Marine Sciences Div. San Diego, CA 91232	1